Accepted Manuscript

Title: Low mass fraction impregnation with graphene oxide (GO) enhances thermo-physical properties of paraffin for heat storage applications

Authors: D. Dsilva Winfred Rufuss, S. Iniyan, L. Suganthi, P.A. Davies

PII: S0040-6031(17)30174-0
DOI: http://dx.doi.org/doi:10.1016/j.tca.2017.07.005
Reference: TCA 77787

To appear in: *Thermochimica Acta*

Received date: 5-5-2017
Revised date: 6-7-2017
Accepted date: 9-7-2017

Please cite this article as: D.Dsilva Winfred Rufuss, S.Iniyan, L.Suganthi, P.A.Davies, Low mass fraction impregnation with graphene oxide (GO) enhances thermo-physical properties of paraffin for heat storage applications, Thermochimica Actahttp://dx.doi.org/10.1016/j.tca.2017.07.005

LOW MASS FRACTION IMPREGNATION WITH GRAPHENE OXIDE (GO) ENHANCES THERMO-PHYSICAL PROPERTIES OF PARAFFIN FOR HEAT STORAGE APPLICATIONS

D. Dsilva Winfred Rufuss[1], S. Iniyan[1], L. Suganthi[2] and P. A. Davies[3]*

[1]Institute for Energy Studies, Department of Mechanical Engineering, College of Engineering Guindy, Anna University, Chennai-600025, India

[2]Department of Management Studies, College of Engineering Guindy, Anna University, Chennai-600025, India

[3] Aston Institute of Materials Research, School of Engineering and Applied Science, Aston University, Birmingham B4 7ET, UK

* Corresponding author: p.a.davies@aston.ac.uk

Graphical Abstract

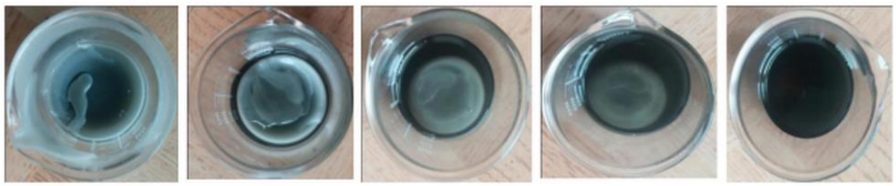

a. Melting images of lower mass fraction GONP impregnated in paraffin

b. Solidification images of lower mass fraction GONP impregnated in paraffin

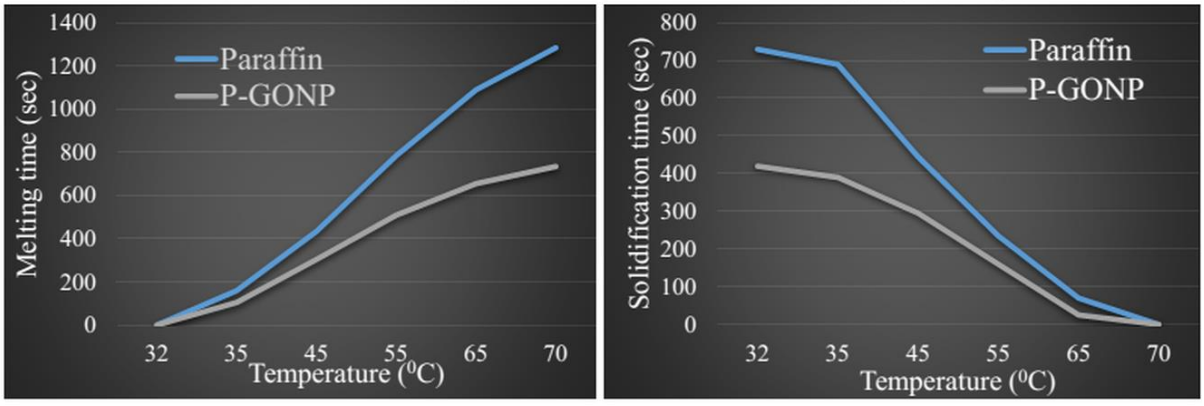

Highlights

- Thermo-physical analysis of lower mass fraction P-GONP nanocomposites is performed
- 101.2 and 94.5% rise in thermal conductivity in solid and liquid state respectively
- Stability and reliability are improved in lower mass fraction P-GONP nanocomposites
- Lower mass fraction and higher mass fraction P-GONP are compared

- Lower mass fraction P-GONP is advantageous from a techno-economic viewpoint

ABSTRACT

Whereas previous researchers analyzed the thermal behavior of paraffin waxes impregnated with graphene oxide nanoparticles (P-GONP) at high mass fraction (>1%), this paper analyzes behavior and stability at only 0.3% mass fraction. GONP was prepared by Hummer's method. The morphology was studied using scanning electron microscope (SEM), transmission electron microscope (TEM), X-Ray diffraction (XRD) and Fourier Transformation-Infrared (FT-IR) Spectrometer and the thermal properties were measured using laser flash analyser (LFA), differential scanning calorimetry (DSC), thermo-gravimetric analysis (TGA) and thermal cycling. LFA showed a 101.2% and 94.5% increase in the thermal conductivity of P-GONP compared to pure paraffin (P) in solid and liquid state respectively. Melting and solidifying temperatures and latent heat were found to be 63.5, 59 °C & 102 kJ/kg and 57.5, 56 °C & 64.7 kJ/kg for P and P-GONP respectively. Thermal cycling over 4000 cycles showed that P-GONP was 27% more stable than P. The latent heat was 64.7 kJ/kg, a 36.5% deterioration compared to virgin paraffin. Compared against higher mass fraction impregnation, lower mass fraction P-GONP was found to have almost equivalent thermo-physical properties (namely thermal conductivity, melting and solidifying characteristics, thermo-chemical stability and reliability) while providing considerable cost saving.

Abbreviations:

Symbols	Abbreviation
DSC	Differential scanning calorimetry
FT-IR	Fourier Transformation-Infrared Spectrometer
GONP	Graphene oxide nanoparticles
JCPDS	Joint Committee on Powder Diffraction Standards
LFA	Laser flash analyser
LHES	Latent heat energy storage

***Keywords*:** phase change material; paraffin; graphene oxide; thermal properties; stability

P	Paraffin
PCM	Phase change material
P-GONP	Paraffin impregnated with graphene oxide nanoparticles
SDBS	Sodium dodecylbenzene sulfonate
SEM	Scanning electron microscope
TEM	Transmission electron microscope
TGA	Thermo-gravimetric analysis
XRD	X-Ray diffraction

1. INTRODUCTION

Energy storage plays a significant role in various applications like energy conversions in buildings, solar thermal technologies and industrial waste heat recovery. Among various energy storage materials, phase change materials (PCM) are very popular for latent heat thermal energy storage (LHTES) owing to their energy density and pre-defined working temperatures. There are various LHTES materials available and their properties have been extensively investigated [1-6]. Among the various LHTES material paraffin is the most popular PCM because of its nucleating behavior, thermo-chemical stability, low vapour pressure, ready availability, good latent heat and cheaper cost. However paraffin is found to be unfit for some applications because of its low thermal conductivity [5-8]. Research is being carried out into various techniques including attaching fins, soaking of porous material and attaching of metal screens/matrix to improve the thermal conductivity and heat transfer rate of paraffin. However these technique increases the weight and volume of the parent or base material i.e. in this case paraffin.

Impregnation of base material with high thermal conductivity materials is a new technique that avoids deterioration in the weight/volume ratio. Various materials such as titanium, zinc, copper, aluminum, and silver have been impregnated into paraffin. Forms of graphite have also been used, such as graphite matrix, porous graphite matrix, expanded graphite, exfoliated graphite

nanoplatelets, exfoliated graphite, graphene (discovered in the year 2004), graphene oxide available which results in distinct/different properties enhancement/deterioration when impregnated in the base material. Researchers have attempted to impregnate nanoparticles in various mass fractions in paraffin. If the mass fraction of nanoparticles in paraffin is less than 1%, it is considered to be low mass fraction; while if it is more than 1%, it is generally referred to as high mass fraction. Literature related to impregnating various mass fractions of different forms of graphite in paraffin is reviewed next.

Py et al. [9] initiated this line of research in the year 2001 by incorporating 5% mass fraction of porous graphite matrix in paraffin and achieved an enhancement in thermal conductivity and thermal stability. The study found that the addition of graphite matrix to paraffin decreases the solidification time. Mills et al. (2006) [10] improved 20-130 times the thermal conductivity of paraffin by impregnating it with the lower mass fraction (less than 1% weight) of graphite matrix. In the same year, Zhang and Fang [11] investigated the thermal properties of paraffin impregnated with expanded graphite (no data were provided about the volume or weight% of impregnation). It was inferred that there was a reduction in phase change temperature of the new composite than that of the virgin paraffin. Sari and Karaipekli (2007) [12] impregnated higher mass fraction (2-10 weight%) expanded graphite in paraffin and found an improvement in thermal conductivity. Thus it is found that the thermal conductivity increases with the impregnation of higher and lower mass fraction nanoparticles. However, this in turn leads to an increase in the total cost of the system.

Kim and Drzal (2009) [13] investigated the latent heat storage capacity and thermal conductivity of paraffin impregnated with higher mass fraction (1-7% weight) of exfoliated graphite platelets and it was found that there was a shift in phase change temperature. Thermal properties such as latent heat, thermal conductivity cannot be extrapolated as it varies non-linearly with the percentage doping of nanoparticles. Hence this study revealed that, though extrapolation of thermal properties could be attempted, it may not be accurate. Besides incurring a cost penalty, the higher weight percentage impregnation of nanoparticles results in agglomeration and causes defects in the lattice arrangements.

Xiang and Drzal (2011) [14] reported that impregnating higher mass fraction (2-8 % mass) of graphite nanoplatelets in paraffin results in the improvement in thermal stability and thermal conductivity as compared to pure paraffin (P). Shi et al. (2013) [15] investigated the shape stabilization and thermal conductivity of paraffin impregnated with higher mass fraction (10% mass) exfoliated graphite nanoplatelets and found that the thermal conductivity increases also helping the base material to become more shape stabilized as compared to the virgin material. The researchers have stated that further research can be done with lower mass fraction of nanoparticles impregnated in paraffin. Very few studies in the literature reports about the thermal behavior of paraffin with graphene oxide nanoparticles

Mehrali et al. (2013) [16] analyzed the thermal conductivity after impregnation with a very high mass fraction (52.2, 52.61, 55.19, 51.7% mass) of graphene oxide in paraffin obtaining an enormous increase of about 223% in thermal conductivity. There was also a reduction in melting and freezing temperature. Nonetheless, such high mass fraction is likely to be prohibitive for most

applications (500 mg of graphene oxide powder costs around $430 as the time of writing). The behavior of paraffin PCM with minimal GO content therefore needs investigation.

The present study aims to address this research gap by providing a comprehensive investigation about the thermal properties of paraffin impregnated with lower mass fraction (0.3% weight) of graphene oxide nanoparticles. As GONP is synthesized at lab scale, it is important to analyze the surface morphology, size, chemical composition and structure of GONP using like SEM, TEM, XRD, FT-IR to confirm the presence of graphene in oxidized form. Thermal behavior like thermal conductivity, phase change temperature, melting and solidification characteristics, thermal reliability and thermal stability of impregnating lower mass fraction of graphene oxide nanoparticles in paraffin are investigated. The reported research also helps to compare the lower mass fraction impregnation studies with the already available higher mass fraction impregnation studies. The paper is presented in the following manner: preparation of nanoparticles, nanocomposites and analysis methods are discussed in section 2. Section 3 covers the results and discussion which includes characterization of the nanocomposites, variations in thermal properties (i.e., thermal stability, reliability, melting & solidification characteristics, thermal conductivity and latent heat). Finally, section 4 presents the conclusions.

2. MATERIALS AND METHODS

2.1 Preparation of nanoparticles

Hummer's method was adopted for the preparation of GO nanoparticles [16-18]. Graphite powder (1g) was mixed with sulfuric acid (H_2SO_4) and stirred until the graphite powder disperses evenly. Potassium permanganate ($KMnO_4$) was gradually added to the solution. The solution was stirred continuously (at 40 °C) for about 12 hours. 100 ml of 2D water was added slowly for dilution and the temperature was rapidly increased to 100 °C and further diluted with 300 ml of water. Hydrogen peroxide (15 ml) of was added to terminate the reaction. The resulting GO was centrifuged and cleansed with hydrochloric acid and deionized water five times and then the sample was dried at room temperature to obtain graphene oxide nanoparticles. The chemical reaction involved in the preparation of GO nanoparticles is depicted in.

Insert Fig. 1. Chemical reaction involved in the preparation of GONP

2.2 Preparation of nanocomposites

As proposed by Harikrishnan et al. [19, 20], an optimum weight percentage of nanoparticles is to be added with the base material in order to avoid agglomeration, reduction in the span of nanocomposites and avoid defects in the lattice structure. In this study, 0.3% weight of the prepared GO nanoparticles was impregnated in paraffin (P) and the physical properties of P is tabulated in Table. 1 and 2. The impregnation ratio of nanoparticles in paraffin was 0.3:100 (i.e. 0.3 g of GONP per 100 g of paraffin). Sodium dodecylbenzene sulfonate (SDBS) was used as a capping agent to get a homogenous dispersion of nanoparticles in paraffin. The preparation process was done in an ultrasonic vibrator (operating at 40 kHz frequency) for 45 min was left for the samples. Longer ultrasonication (more than 60 min) will lead to lattice deformation and causes various defects in nanocomposites [21, 22]. The ultrasonic vibrator was maintained at 70 °C

(approximately 5 °C above the melting point of paraffin) which was sufficient for keeping the sample in liquid state throughout the nanocomposite preparation process. According to the hypothesis developed by He et al. [23] for GO and [24] for paraffin, the chemical structure of paraffin impregnated with GO nanoparticles is depicted in Fig. 2.

Insert Table 1. Thermal conductivity and % increase in thermal conductivity of P and P/GONP

Insert Table 2. Latent heat, melting and solidifying temperature of P and P/GONP

Insert Fig. 2. Chemical structure of P-GONP

2.3 Analysis methods

A Carl Zeis MA15/ EVO 18 scanning electron microscope (SEM), Germany was used to analyze the surface morphology of the samples. The magnification and resolution of the SEM instrument was 50K ~ 100K and ~ 50 nm. To prepare the samples, sputtering was carried out using 10-nm size gold-palladium (Au/Pd) nanoparticles for 20 s. The extra-high voltage (EHT) source of about 20 kV was first tested and adjusted on high-thermal conductivity self-organized patterned gold samples. Pressure was maintained at 10 Pa during these experiments. The instrument was operated with a secondary electron detector of tungsten at 30 kV. To reduce beam damage, a backscatter electron detector (BSD) was used with the sample tilted at 70° to the horizontal. The field of view was 6 mm from the working distance, and the take-off angle for X-ray analysis was 35°. A CM-120-Philip transmission electron microscope (operating voltages 20, 40, 60, 80 and 100 kV) was used to visualize the dispersion and measure the size of nanoparticles. Lanthanum hexa-bromide (LaB6) filament was used as the beam source. The goniometer was fully computer controlled over ±70°. Cooling was with liquid nitrogen. Auto-calibration was done periodically after multi-sample measurements to ensure the accuracy of the results.

The chemical structural analysis was done with Fourier Transformation- Infrared (FT-IR) Spectrometer (Bruker Alpha) with the range of about 3500-500 cm^{-1}. The signal-to-noise ratio of the instrument was 50000:1 with measurement time and spectral resolution of about 1 min and 4 cm^{-1} respectively. A deuterated and L-alanine-doped tri-Glycine sulfate (DLaTGS, Curie temperature 61 °C) pyroelectric device was used as the thermal detector; and $LiTiO_3$ was used as the pyroelectric detector. The latent heat, melting and solidification point of the sample were measured using differential scanning calorimetry (Perkin Elmer-DSC 4000 series, USA; frequency 50-60Hz) whose temperature range is -100 to 450 °C and heating rate is 5 °C/min. The accuracy and precision of the DSC instrument were ±2% and ±0.1% respectively. The furnace material was aluminium coated with alumina. A nickel-chromium thermocouple (90% Ni and 10% Cr) was used to measure the temperatures. For the calorimetry, 1 mg of indium at 10 °C/min with nitrogen purge was used. Three types of calibration – temperature calibration, furnace calibration and heat flow calibration – were carried out using the instrument viewer and the method editor. The digital resolution and melting time for the indium was 0.02 μW and 3.3 s respectively. The sample mass was 3 mg and the cooling rate was 5 °C/min.

The thermal stability of the sample was tested using a thermogravimetric analyzer (PerkinElmer, USA, Model Diamond TG/DTA) with operating temperature up to 900 °C and

heating rate of about 20 °C/min. The maximum operating temperature and heating rate of the instrument were 1500 °C and 0.01-100 °C/min respectively. The sample mass of 4 mg was placed in a ceramic crucible pan, calibrated using PYRIS software version 7.0.0.0110. The thermal decomposition of the sample was measured using the difference in the weight of the sample and reference pans. The cooling was done by a microprocessor controlled cooling fan controlled by PYRIS software. Nitrogen was used as the purge gas with flow rate of about 20 ml/min.

X-ray diffraction was carried out using Shimatzu diffractometer X-ray XRD 6000 model, Japan, with scattering angle (2θ) between 20° to 80°. The crystal size was calculated by line broadening with Debye-Scheree's relation ($D=0.99\lambda/W \cos\theta$, where λ and W correspond respectively to the wavelength of the X-ray and full width at half maximum). A calibration curve was generated between intensity and integrated intensity. The scanning radius of the goniometer was 185 mm and the minimum step angle was 0.002°. CuK_{α} radiation was used in the analysis. The sample mass was 2 g. A scintillation counter was used as a detector, with NaI as the scintillator material. The thermal reliability of the sample was tested consecutively up to 4000 thermal cycles using a thermal cycler- BIOER TC-25/H model. The heating and cooling rates were 3 and 2 °C/s respectively. The temperature range and accuracy of the instrument were 4-99 °C and ±0.5 °C respectively. The temperature of the hot lid was maintained at 105 °C. The thermal conductivity of the sample was measured using a LFA 467 HyperFlash-Light Flash Apparatus (Germany) with temperature range of about -100 °C to 500 °C. The thermal conductivity and thermal diffusivity ranges of this instrument were 0.1-4000 W/m°C and 0.01-2000 mm^2/s respectively and its maximum heating rate was 50 °C /min. The accuracy and repeatability of thermal diffusivity was ±3% and ±2% respectively. The pulse energy and pulse width of the xenon flash lamp was up to 10 J/pulse and 20-1200 μs respectively. The accuracy and repeatability of specific heat capacity measurement was ±5% and ±3% respectively. Liquid nitrogen was used to cool the furnace. The vacuum was maintained at less <150 mbar. Pulse mapping and temperature detection were as associated with the 2 MHz data acquisition system.

3. RESULTS AND DISCUSSION

3.1 Characterization of P and P-GONP

The FT-IR spectra of paraffin is depicted in Fig. 3. The region between 3000-2850 cm^{-1} (2800.84, 2849.78 and 2916.59) corresponds to stretching vibration of C-H bond for aliphatic and methyl group and the region 1465.45 cm^{-1} corresponds to methylene group [25]. The FT-IR spectra of the prepared P-GONP is depicted in Fig. 4. From the figure, the peak at 1748 .67, 1526.25, 1357.74, 960.02 and 2916.68 cm^{-1} indicates the presence of carboxyl C=0, aromatic C=C, epoxy C-O, alkoxy C-O and $–CH_3$ group respectively and hence this confirms that the graphite was oxidized into GO [24]. The XRD pattern of P-GONP is depicted in Fig. 5. The diffraction peak (2θ) was noted at 9.7 which confirms the presence of graphene oxide (JCPDS file no: 41-1487) [26]. The surface morphology and size of the nanoparticles are measured using SEM and TEM. The surface morphology of P-GONP is depicted in Fig. 6 and the TEM image is depicted in Fig. 7. From the results, it is noted that, a homogenous dispersion of GONP in P was observed and the P-GONP has folded foil shape (3D). This homogenous dispersion may be because of the surfactant used during the preparation of P-GONP. The range of nanoparticles was between 20 to 100 nm. Very

slight aggregation was observed in the corner. This will not cause any deviation in thermal behaviour of P-GONP. Thus Fourier Transformation- Infrared (FT-IR) Spectrometer, X-ray diffraction, SEM and TEM results confirms the presence of paraffin and GONP in paraffin.

Insert Fig. 3. FT-IR spectra of Paraffin

Insert Fig. 4. FT-IR spectra of P-GONP

Insert Fig. 5. XRD pattern of P-GONP

Insert Fig. 6. SEM image of P-GONP

Insert Fig. 7. TEM image of P-GONP

3.2 Thermal stability and reliability of P-GONP

Once the characterization of nanocomposites was completed, the thermal stability of the composites was tested to find the degradation temperature range and peak degradation point using thermogravimetric analysis. The thermogravimetric curves of P and P-GONP are depicted in Fig. 8. The degradation temperature of the base material (paraffin) was in the range 130-180 °C. When GONP are impregnated to the base material the degradation temperature range increased to 165-298 °C. The percentage increase in the stability of P-GONP was found to be 26.9% than that of the base material (P). This may be due to the bond breakage of polymers into monomers. The peak degradation points for P and P-GONP were found to be 232 and 268 °C respectively. Hence it is evident that P-GONP showed improved thermal stability than that of virgin paraffin. The graph depicting the thermal reliability of the samples with the phase change temperature against the number of cycles during charging and discharging period is shown in Fig. 9. The shift of melting and solidification temperature was found to be -1.559, -2.07% and -1.866, -0.179% for P and P-GONP respectively and hence this will not cause any consequence to the energy storage system. Thus it is confirmed that the impregnation of GONP in P improved the thermal stability and reliability of virgin paraffin.

Insert Fig. 8. TGA curves of paraffin

Insert Fig. 9. Thermal reliability of P and P-GONP

3.3 Thermal behavior of P-GONP

There are two main parameters which influence the melting and solidification characteristics of PCM. They are melting and solidification temperature, and melting and solidification time. The variation in melting and solidification characteristics of P and P-GONP is depicted in Fig. 10 and 11 and tabulated in Table. 2. There was a decrease in melting and solidification temperature observed in P-GONP compared to virgin paraffin. The melting temperature of pure paraffin was found to be 63.5 °C and when GONP was impregnated in paraffin the melting point decreased to 57.5 °C. A similar behavior was observed in solidification temperature. The solidification temperature of pure paraffin was 59 °C and when GONP was impregnated, the solidification temperature decreased to 56 °C. To summarize, the GONP have a tendency to reduce the melting and solidification temperature than that of pure paraffin.

Insert Fig. 10. DSC curves of Paraffin

Insert Fig. 11. DSC curves of P-GONP

When the present results are compared with the results obtained by impregnating very high mass fraction of GONP in paraffin (Mehrali et al. [16]), it is found that the melting temperature of virgin paraffin was 53.5 °C and when 52.6 weight% was impregnated with virgin paraffin the melting temperature decreases to 52.33 °C respectively. In the present research when 0.3 weight% of GONP is impregnated in paraffin the melting temperature decreases from 63.5 to 57.5 °C. Thus with 0.3 weight% impregnation, 9.44% decrease in melting point is achieved but whereas when 52.61 weight% is impregnated there was only 2.11% decrease. Thus with smaller mass fraction impregnation of GONP in paraffin gives comparatively good results for substantial cost reduction.

Melting and solidification time is also an important phenomena that needs to be considered for investigating the charging and discharging characteristics of PCM. The melting time of the base material reduces with the addition of nanoparticles. The variation of melting time with respect to temperature of P and P-GONP is depicted in Fig. 12. The percentage time savings for P-GONP for complete melting was found to be 42.80% as compared to pure paraffin. The time taken for complete melting of P and P-GONP was found to be 1285 and 735 sec respectively. The variation of solidification curve with respect to temperature of P and P-GONP is depicted in Fig. 13. It is clear that the time taken for complete solidification of paraffin was higher than that of P-GONP. The percentage time savings in solidification time of P-GONP was found to be 42.46% as compared to virgin paraffin. The time taken for complete solidification for P and P-GONP was found to be 730 and 420 sec respectively. The images of complete melting and solidification process of P-GONP is depicted in Fig. 14.a and Fig. 14.b respectively. Thus the addition of nanoparticles increases the discharging period of the base material.

Insert Fig. 12. Melting characteristics of P and P-GONP showing faster melting of P-GONP

Insert Fig. 13. Solidification characteristics of P and P-GONP showing faster solidification of P-GONP

Insert Fig. 14. Complete melting and solidifying process of P-GONP

3.4 Latent heat of P-GONP

The variation in latent heat of P and P-GONP was measured using DSC analysis. The values have already been tabulated in Table. 2. The latent heat of paraffin (base material) was found to be 102 kJ/kg and an interesting characteristic was observed when GONP is impregnated, i.e. P-GONP showed decrement in latent heat than that of the virgin paraffin. The latent heat of P-GONP was found to be 64.7 kJ/kg. There was 36.5% decrease in latent heat observed in P-GONP than that of virgin paraffin. This may be due to carbon and oxygen bond arrangement in structural lattice, hydrophilic material, sp^2 hybridization, aggregation property, dispersing property with organic solvents, molecular sieves and organic covalent functionalization of graphene oxide. This purely depends on the type of nanoparticles and base material. However the property may vary according to the impregnated % of GONP in paraffin as against virgin paraffin.

When the latent heat of lower mass fraction impregnation of GONP in paraffin is compared with the higher mass fraction impregnation (Mehrali et al. [16]), there was an increase in the latent heat of lower mass fraction impregnation of GONP in paraffin than that of higher mass fraction. The comparison is tabulated in Table. 3. With 0.3% impregnation, almost similar results are obtained as of 52.2 weight% of impregnation. Hence lower mass fraction of GONP in paraffin can used. Higher mass fraction of GONP impregnation in paraffin lowers the latent heat and decreases the latent heat energy storage capacity of virgin paraffin.

Insert Table. 3. Comparison of lower mass fraction impregnation and higher mass fraction impregnation of GONP in paraffin

3.5 Thermal conductivity of P-GONP

The thermal conductivity of P and P-GONP is depicted in Fig. 15. The thermal conductivity of virgin paraffin at solid and liquid state was found to be 0.26 and 0.164 W/mK respectively. The percentage increase in thermal conductivity of P and P-GONP have already been tabulated in Table. 1. The impregnation of GONP in paraffin increased the thermal conductivity of P-GONP from 0.26 to 0.523 W/mK at solid state and from 0.164 to 0.319 W/mK at liquid state. At solid state, there was 101.1 percentage increase in the thermal conductivity observed for P-GONP than that of base paraffin. At liquid state, the percentage increase in thermal conductivity was found to be 94.5% for P-GONP than that of pure paraffin. Hence it is concluded that there is a significant improvement observed in the thermal conductivity of P-GONP as against to the virgin paraffin.

Insert Fig. 15. Thermal conductivity of P and P-GONP

When the thermal conductivity of lower mass fraction impregnation of GONP in paraffin is compared with the higher mass fraction impregnation (Mehrali et al. [16]), it is found that there is less improvement in the thermal conductivity of higher mass fraction impregnation than that of the lower mass fraction impregnation (Table. 3). When 0.3 weight% GONP is impregnated in paraffin there was 100% improvement in thermal conductivity whereas when 52.2 weight% of GONP is impregnated in paraffin there was only around 200% improvement in thermal conductivity. Similar results were achieved by impregnating expanded graphite and exfoliated graphite nanoplatelets in paraffin, by Sari and Karaipekli (2007) [12] and Shi et al. (2013) [15] respectively. The thermal conductivity of various mass fractions of graphite nanoparticles impregnated in paraffin is depicted in Fig. 16. It is inferred from the Figure that the thermal conductivity increases as the mass fraction of nanoparticles increases. Thus, depending on the application requirement the percentage impregnation may be decided considering the cost of the system.

Insert Fig. 16. Thermal conductivity enhancement in paraffin impregnated with various forms of graphite

3.6. Cost of various forms of graphite

The cost of various forms of graphite i.e, graphene oxide, graphene nanoplatelets and reduced graphene oxide is 168 $/gm, 906 $/gm and 108 $/gm respectively [27] and [28]. The cost increases linearly with the mass of nanoparticles required. The studies by Mehrali et al. [16], focus

on higher mass fraction impregnation of GO in paraffin which has good thermo-physical properties but may incur severe cost penalty during commercialisation. Hence to reduce the total cost of the system, the mass fraction of GONP for impregnation should be reduced. From the results discussed above, lower mass fraction impregnation of GONP in paraffin appears viable both technically and economically.

4. CONCLUSION

A new P-GONP composite PCM was prepared by impregnating low mass fraction (0.3 %) of graphene oxide nanoparticles in paraffin. The characterization of nanocomposites was performed using SEM, TEM analysis, XRD analysis and FT-IR spectra, confirming presence of graphene in oxidized form. Thermal properties of stability, conductivity, phase change temperatures and latent heat were measured using TGA, LFA and DSC analysis. Based on the results, the following conclusions were drawn:

P-GONP is much more stable than virgin paraffin showing an improvement of about 27% in thermal cycling and gravimetric tests. The melting and solidification temperatures reduced to 57.5 °C and 56 °C respectively, compared to 63.5 °C and 59 °C respectively for virgin paraffin. P-GONP also showed better charging and discharging rates, decreased by 42.8 and 42.5% respectively compared to virgin paraffin. And P-GONP showed improved thermal conductivity over that of virgin paraffin giving a 101.1 and 94.5% increase in solid and liquid state respectively. In contrast, a 36.5% deterioration was observed in the latent heat of P-GONP. The decrease in latent heat was modest when compared to the tremendous increase in thermal conductivity of P-GONP. When lower mass fraction is compared to higher mass fraction impregnation of GONP in paraffin, lower mass fraction impregnation gave superior results overall.

Hence, it is concluded that the prepared lower mass fraction (<1%) P-GONP composite (prepared by impregnating lower mass fraction of graphene oxide in paraffin) is favorable from a techno-economic view. It can hence be used for LHTES application due to its improved thermo-chemical stability, reliability, charging and discharging rate and thermal conductivity – with minimal cost penalty.

Acknowledgements

The authors gratefully acknowledge the Department of Science and Technology and British Council for providing financial support under the UKIERI programme (DST/INT/UK/P-86/2014). One of the authors, Mr. Dsilva Winfred Rufuss D, also gratefully acknowledges support received under the Maulana Azad National Fellowship (MANF), University Grants Commission (UGC), India.

Reference

[1] A. Abhat, Low temperature latent thermal energy storage system: heat storage materials, Sol. Energy 30 (1983) 313–332.
[2] I. Dincer, M.A. Rosen, Thermal Energy Storage, Systems and Applications, Wiley, England, 2002.
[3] K. Kaygusuz, The viability of thermal energy storage, Energy Sour. 21 (1999) 745–756.

[4] A. Sarı, Thermal characteristics of a eutectic mixture of myristic and palmitic acids as phase change material for heating applications, Appl. Therm. Eng. 23 (2003) 1005–1017.
[5] S.D. Sharma, K. Sagara, Latent heat storage materials and systems: a review, Int. J. Green Energy 2 (2005) 1–56.
[6] B. Zalba, J.M. Marin, L.F. Cabeza, H. Mehling, Review on thermal energy storage with phase change: materials, heat transfer analysis and applications, Appl. Therm. Eng. 23 (2003) 251–283.
[7] S. Himran, A. Suwono, G.A. Mansoori, Characterization of alkanes and paraffin waxes for application as phase change energy storage medium, Energy Sour. 16 (1994) 117–128.
[8] D.D.W. Rufuss, S. Iniyan, L. Suganthi, P.A. Davies, Solar stills: A comprehensive review of designs, performance and material advances, Renew. Sust Energy Rev. 63 (2016): 464-496.
[9] X. Py, S. Olives, S. Mauran, Paraffin/porous graphite matrix composite as a high and constant power thermal storage material, Int. J. Heat Mass Transf. 44 (2001) 2727–2737.
[10] A. Mills, M. Farid, J.R. Selman, S. Al-Hallaj. Thermal conductivity enhancement of phase change materials using a graphite matrix, Appl. Therm. Eng. 26 (2006) 1652-1661.
[11] Z. Zhang, X. Fang. Study on paraffin/expanded graphite composite phase change thermal energy storage material, Energy Convers. Manage. 47 (2006) 303-10.
[12] A. Sarı, A. Karaipekli. Thermal conductivity and latent heat thermal energy storage characteristics of paraffin/expanded graphite composite as phase change material, Appl. Therm. Eng. 27 (2007) 1271-7.
[13] S. Kim, L.T. Drzal. High latent heat storage and high thermal conductive phase change materials using exfoliated graphite nanoplatelets, Sol. Energy Mater. Sol. C. 93 (2009) 136-42.
[14] J. Xiang, L.T. Drzal. Investigation of exfoliated graphite nanoplatelets (xGnP) in improving thermal conductivity of paraffin wax-based phase change material, Sol. Energy Mater. Sol. C. 95 (2011) 1811-8.
[15] J.N. Shi, M.D. Ger, Y.M. Liu, Y.C. Fan, N.T. Wen, C.K. Lin, N.W. Pu. Improving the thermal conductivity and shape-stabilization of phase change materials using nanographite additives, Carbon. 51 (2013) 365-72.
[16] M. Mehrali, S.T. Latibari, M. Mehrali, H.S. Metselaar, M. Silakhori. Shape-stabilized phase change materials with high thermal conductivity based on paraffin/graphene oxide composite, Energy Convers. Manage. 67 (2013) 275-82.
[17] W. Yu, H. Xie, D. Bao. Enhanced thermal conductivities of nanofluids containing graphene oxide nanosheets, Nanotechnology 21 (2009) 055705.
[18] W. Yu, H. Xie, W. Chen. Experimental investigation on thermal conductivity of nanofluids containing graphene oxide nanosheets, J. Appl. Phys. 107 (2010) 094317.
[19] S. Harikrishnan, S. Magesh, S. Kalaiselvam. Preparation and thermal energy storage behavior of stearic acid–TiO_2 nanofluids as a phase change material for solar heating systems, Thermochim. Acta. 565 (2013) 137-145.
[20] S. Harikrishnan, S. Kalaiselvam. Preparation and thermal characteristics of CuO–oleic acid nanofluids as a phase change material, Thermochim. Acta. 533 (2012) 46-55.

[21] B.E. Jebasingh. Exfoliation of graphite by solar irradiation and investigate their thermal property on capric–myristic–palmitic acid/exfoliated graphite composite as phase change material (PCM) for energy storage, Journal of Energy Storage. 5 (2016) 70-76.
[22] M.J. O'Connell, S.M. Bachilo, C.B. Huffman. Band gap fluorescence from individual single-walled carbon nanotubes, Science 297 (2002) 593–596.
[23] He, H.; Klinowski, J.; Forster, M.; Lerf, A. (1998). "A new structural model for graphite oxide". Chemical Physics Letters. **287**: 53.
[24] Study on demulsifier formulation for treating Malaysian crude oil emulsion - Scientific Figure on ResearchGate. Available from: https://www.researchgate.net/44707616_fig3_Figure-25-Average-structure-of-paraffin-wax-molecule-Mussen-1998 [accessed 12 Apr, 2017]
[25] K.J. Arun, A.K. Batra, A. Krishna, K. Bhat, M.D. Aggarwal, J.P. Francis. Surfactant Free Hydrothermal Synthesis of Copper Oxide Nanoparticles, American Journal of Materials Science 5 (2015) 36-38.
[26] Y. Pan, K. Ye, D. Cao, Y. Li, Y. Dong, T. Niu, W. Zeng, G. Wang. Nitrogen-doped graphene oxide/cupric oxide as an anode material for lithium ion batteries. RSC Adv. 110 (2014) 64756-62.
[27] http://www.sigmaaldrich.com/materials-science/material-science-products.html?TablePage=112007852 (accessed 12-04-2017)
[28] http://www.sigmaaldrich.com/materials-science/material-science-products.html?TablePage=20907802 (accessed 12-04-2017).

Table 1. Thermal conductivity and % increase in thermal conductivity of P and P/GONP

Table 2. Latent heat, melting and solidifying temperature of P and P/GONP

Table. 3. Comparison of lower mass fraction impregnation and higher mass fraction impregnation of GONP in paraffin

List of figure caption

Fig. 1. Chemical reaction involved in the preparation of GONP

Fig. 2. Chemical structure of P-GONP

Fig. 3. FT-IR spectra of Paraffin

Fig. 4. FT-IR spectra of P-GONP

Fig. 5. XRD pattern of P-GONP

Fig. 6. SEM image of P-GONP

Fig. 7. TEM image of P-GONP

Fig. 8. TGA curves of paraffin

Fig. 9. Thermal reliability of P and P-GONP

Fig. 10. DSC curves of Paraffin

Fig. 11. DSC curves of P-GONP

Fig. 12. Melting characteristics of P and P-GONP showing faster melting of P-GONP

Fig. 13. Solidification characteristics of P and P-GONP showing faster solidification of P-GONP

Fig. 14. Complete melting and solidifying process of P-GONP

Fig. 15. Thermal conductivity of P and P-GONP

Fig. 16. Thermal conductivity enhancement in paraffin impregnated with various forms of graphite

Table 1.

Thermal conductivity and % increase in thermal conductivity of P and P/GONP

Type of PCM	Thermal conductivity (W/mK)		Percentage increase in thermal conductivity (%)	
	Solid state	Liquid state	Solid state	Liquid state
Paraffin (P)	0.26	0.164	-	-
P/GONP	0.523	0.319	101.1538	94.5122

Table 2.

Latent heat, melting and solidifying temperature of P and P/GONP

Sl.no	Type of PCM	Latent heat (kJ/kg)	Melting temperature (^{0}C)	Solidifying temperature (^{0}C)
1	Paraffin (P)	102	63.5	59
2	P/GONP	64.7	57.5	56

Table. 3.

Comparison of lower mass fraction impregnation and higher mass fraction impregnation of GONP in paraffin

Author	Percentage of GONP impregnated in paraffin	Thermal conductivity (W/mK)		Latent heat (kJ/kg)	Melting temperature (^{0}C)
		Solid state	Liquid state		
Mehrali et al. [16]	0 weight% (virgin paraffin)	0.287	0.305	131.92	53.46
Mehrali et al. [16]	52.2 weight%	0.952	1.04	63.11	54.60
Mehrali et al. [16]	52.61 weight%	0.964	1.19	62.53	51.48
Mehrali et al. [16]	55.19 weight%	1.32	1.45	59.12	52.33
Mehrali et al. [16]	51.7 weight%	0.932	0.985	63.76	53.57
Present study	0 weight% (virgin paraffin)	0.26	0.164	102	63.5
Present study	0.3 weight%	0.523	0.319	64.7	57.5

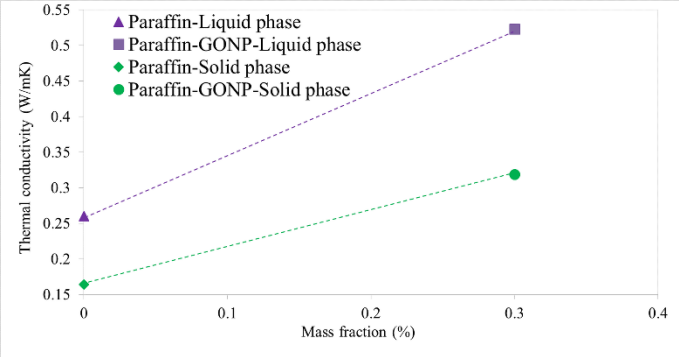

a. Melting images of lower mass fraction GONP impregnated in paraffin

b. Solidification images of lower mass fraction GONP impregnated in paraffin